

Superhydrophobic textures for microfluidics

Olga I. Vinogradova^{*a,b} and Alexander L. Dubov^a

^a A. N. Frumkin Institute of Physical Chemistry and Electrochemistry, Russian Academy of Sciences, 119991 Moscow, Russian Federation. Fax: +7 495 952 5308; e-mail: oivinograd@yahoo.com

^b Department of Physics, M. V. Lomonosov Moscow State University, 119991 Moscow, Russian Federation

DOI: 10.1016/j.mencom.2012.09.001

Superhydrophobic surfaces have opened a completely new field of investigation with both fundamental and practical perspectives. Research on these materials has mostly focused on their extreme non-wettability, which has large-scale implications in the context of self-cleaning and impact processes. However, the implications of superhydrophobicity for transport phenomena, which are especially important at micro- and nanoscales, remain largely unexplored. Here, we summarize recent advances in this field, including the physical causes of water repellency, the origins of superhydrophobicity and a current switch in focus from wetting to related areas such as the remarkable drag-reducing ability of superhydrophobic materials. In particular, we show that superhydrophobic surfaces induce novel hydrodynamic properties such as giant effective slip, superfluidity and mixing, and affect electrokinetic phenomena. We also discuss developments and strategies in the fabrications of superhydrophobic materials for relevant applications, including microfluidic lab-on-a-chip devices. We finally suggest several remaining challenges in the field.

Introduction

Controlling the wettability of solid materials is a key issue in surface engineering, and wetting phenomena have been studied for at least two centuries. If a solid surface is flat, smooth and chemically homogeneous, the equilibrium contact angle is determined by Young's equation

$$\cos \theta = (\gamma_{SV} - \gamma_{SL}) / \gamma_{LV}, \quad (1)$$

where γ_{SV} , γ_{SL} and γ_{LV} are the surface tensions of solid–vapor, solid–liquid and liquid–vapor interfaces, respectively. This contact angle is fixed by the chemical nature of the three phases. In many common situations, this angle lies between 0° and 90° (i.e., a hydrophilic case), but some solids can have a contact angle greater than 90° (a hydrophobic case). However, even on the most hydrophobic solids (fluorinated materials), the contact angle never exceeds 120°. This implies, for instance, that they cannot generate some special properties of obvious practical interest, based on water repellency.

However, only very few solids are molecularly smooth. Conversely, most of them, including surfaces of many plants¹ and animals, are rough being naturally decorated with special micro- and nanotextures. Such a roughness may also be induced by fabrication or coating processes. If these materials are chemically hydrophobic, the presence of a microtexture can dramatically lower the ability of drops to stick due to water repellency or

so-called superhydrophobicity. For these surfaces, the effective water contact angle can exceed 150° (see Figure 1).

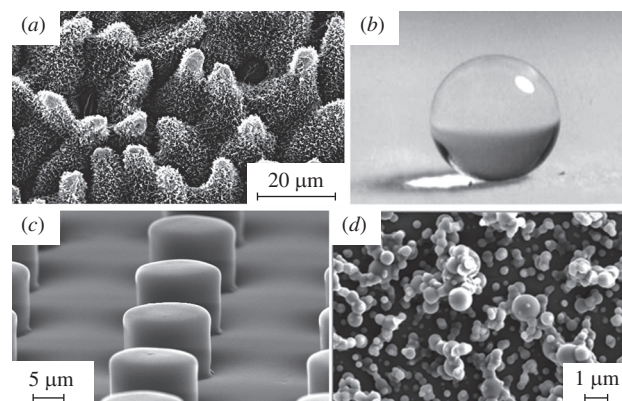


Figure 1 Scanning electron microscopy images of superhydrophobic materials with different textures and a water drop deposited on a superhydrophobic substrate: (a) hierarchical structure of the Lady's Mantle (*Alchemilla diphylla*) leaf (reprinted with permission from ref. 1, © 1997, by Annals of Botany Company); (b) a water drop on a fractal superhydrophobic surface (reprinted with permission from ref. 2, © 1996, by American Chemical Society); (c) patterned array of silica micropillars obtained by nanoimprint lithography (adapted from ref. 3) and (d) randomly rough superhydrophobic surface obtained *via* aerosol assisted chemical vapor deposition (reprinted with permission from ref. 4, © 2009, by The Royal Society of Chemistry).



Olga I. Vinogradova is the head of the Laboratory of Physical Chemistry of Modified Surfaces at the A. N. Frumkin Institute of Physical Chemistry and Electrochemistry (Russian Academy of Sciences) and a professor of the Physics Department at the M. V. Lomonosov Moscow State University. Her main research interests are in the field of 'soft condensed matter' including fluid dynamics, wetting, colloidal interactions, and electrochemical systems motivated by problems in modern micro- and nanofluidics, materials science, energy, biophysics *etc.*

Alexander L. Dubov is a PhD student at the Laboratory of Physical Chemistry of Modified Surfaces at the A. N. Frumkin Institute of Physical Chemistry and Electrochemistry (Russian Academy of Sciences). His PhD project combines the experimental studies and computer (lattice-Boltzmann) simulations of the wetting and hydrodynamic properties of superhydrophobic materials decorated with well-controlled micropillars and microgrooves.



The issue of large contact angle of superhydrophobic materials was first addressed more than 50 years ago being strongly motivated by industrial interest in textile coatings.^{5,6} However, only in the last decade the field is rapidly advanced, not the least due to potential macroscopic applications (that mostly rely on the formation of a stable air–liquid interface) such as self-cleaning materials,^{7,8} non-wetting and anti-fog glass coatings,^{9–12} biomedical devices, optics¹³ *etc.* Thanks to a rapid development of fabrication methods,^{14–16} first of all techniques coming from microelectronics, we are now able to elaborate substrates whose surfaces are patterned (at micro- and nanometer scales) in a very well-controlled way that provided a system to test theoretical ideas. In parallel, a significant progress has been made in the characterization of properties of superhydrophobic surfaces, such as wettability and stability of air trapped within the texture. However, despite a decade of intense research, superhydrophobicity studies were mostly focused on the surface design of new materials and the characterization of their wetting properties. Moreover, these surfaces even designed for wetting purposes still plagued with problems that restrict their practical applications: contact angle hysteresis, fragility under pressure and difficult and/or expensive fabrication.

It is of course important to address remaining challenges in the area of wetting, but today the main research questions become slightly different. Over past few years, the cutting edge in the development of synthetic superhydrophobic surfaces has shifted from wetting towards their greatly enhanced properties that can impact the dynamics of liquids.^{17–19} For instance, due to a very low degree of sticking to superhydrophobic surfaces, the water drop slides²⁰ or rolls with amazingly large velocity, and a drop hitting such a material just bounces off, which is of obvious interest for such applications as waterproof clothes or windshields.⁹ These macroscopic dynamic studies raised a question of a possible large effective slip of water past superhydrophobic materials with trapped gas and its drag-reducing ability, which could be extremely important in microfluidics^{17,18,21,23} – a recently emerged distinct field that requires manipulation of fluids in very thin channels and has the potential to influence subject areas from chemical synthesis and biological analysis to optics and information technology. These new opportunities generated new challenges in the design of superhydrophobic materials and also posed many new fundamental issues to address. For example, the effective contact angle cannot be used for characterizing the dynamic properties of superhydrophobic surfaces, and other physical parameters should be employed to optimize materials for given dynamic applications.^{10,24}

Here, we summarize recent advances in the design of superhydrophobic materials by focusing mostly on new challenges from the past several years. We start with a very brief description of the two states of superhydrophobicity. Then follow the results highlighting the new opportunities related to enhanced transport phenomena and their optimization. In the following section we discuss challenges in the materials design for wetting properties and microfluidic applications with a brief consideration of fabrication methods. We close with some suggestions concerning experimental and theoretical studies in this expanding area of research.

Wetting: the two states of superhydrophobicity

Equation (1) is violated due to irregularities of the superhydrophobic surface. There are two main regimes of wetting of such a surface: either the liquid follows the solid surface, or it leaves air inside the texture.

In the first regime (Wenzel scenario⁵), an increase in the surface area (due to the texture) amplifies the natural hydrophobicity of the material. The key parameter controlling the effective contact angle, $\cos \theta_w$, on this surface is the solid rough-

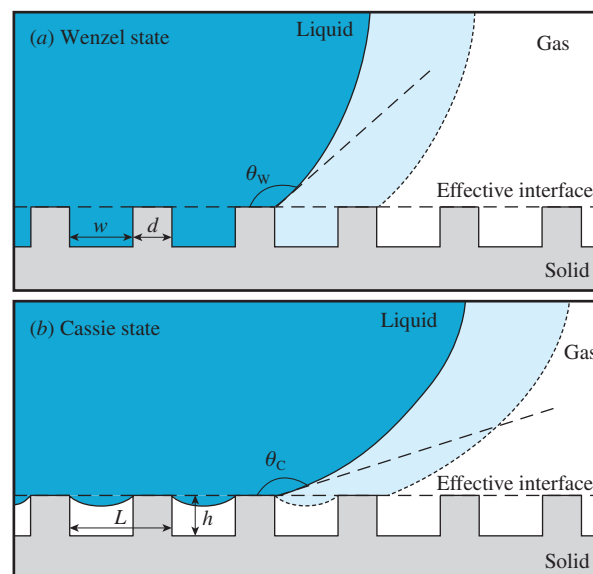


Figure 2 Displacing the contact line in the (a) Wenzel (homogeneous), and (b) Cassie (heterogeneous) regimes.

ness r , defined as the ratio between the actual and apparent surface areas [Figure 2(a)]:

$$\cos \theta_w = r \cos \theta. \quad (2)$$

In what follows that to get a very large effective (Wenzel) contact angle one has to increase the roughness of hydrophobic materials.

In the second state (first described by Cassie and Baxter⁶), the liquid only contacts the solid on the top of asperities, on fraction of surface we denote as φ_s [Figure 2(b)], owing to a trapped air. Assuming that these air pockets have a flat interface with the liquid, we derive the following formula for the effective contact angle:

$$\cos \theta_c = \varphi_s - 1 + \varphi_s \cos \theta, \quad (3)$$

whence the large effective (Cassie) angle is possible only at a very small fraction of the solid–gas interface.

Since most of the ‘super’ properties of superhydrophobic surfaces are due to the air trapped within the texture, the Cassie state is often more desirable than the Wenzel state.^{25–28} During the last decade, much insight has been gained into the relative stability of the Cassie state, the Cassie-to-Wenzel transition,^{9,22,25–27,29–31} which can occur for a number of reasons, such as an increase in pressure, evaporation, external forces or the presence of surface defects.^{32–34} This characterization of the wetting properties has been addressed with experiments, theory²⁷ and computer simulations.³⁵

Most of approaches were based on thermodynamic (energy) arguments. A comparison between the surface energies of the Wenzel and Cassie states (by assuming the liquid–air interface to be flat) suggests that stable air pockets are only possible when hydrophobicity is large enough, *i.e.*, at $\theta > \theta_{cr}$, where

$$\cos \theta_{cr} = (1 - \varphi_s)/(r - \varphi_s). \quad (4)$$

The more advanced energy approach takes into account the curvature of meniscus:³⁶

$$(\gamma + h\Delta p) \cos \theta_{cr} - \gamma \cos \theta > 0, \quad (5)$$

where h is the texture height, and Δp is the capillary pressure. One of the startling implications of these studies is that the stable Cassie state is possible even at some hydrophilic textures (*e.g.*, mushroom-shaped pillars *etc.*^{30,37}).

For very dilute textures, the energy conditions cannot be fulfilled owing to the limitations on chemical hydrophobicity. In this situation, the Cassie state should generally be metastable, and the transition to the Wenzel state happens when the bottom interface of the drop contacts the ground level of the texture.^{28,38}

Note that the actual fractions of solids in contact with the liquid are unknown for arbitrary rough or fractal surfaces, so that one can normally get only a qualitative agreement with theoretical models. Over a decade to go further surfaces with the controlled design of periodic roughness have been intensively used.³⁹ Note that r or φ_S are no longer adjustable parameters, but they can be precisely calculated from known texture parameters, such as height h , diameter d and distance w (see Figure 2). For example, for a surface decorated by an array of rectangular pillars, one can easily evaluate $r = 1 + 4dh/L^2$ and $\varphi_S = d/L$, where $L = w + d$ is the period of the texture. Correspondingly, for a grooved surface, we get $r = 1 + h/L$ and $\varphi_S = d/L$. Thus, they can vary largely for a given texture. In efforts to better understand the connection between the texture parameters and the stability of the Cassie state, the Cassie-to-Wenzel transition has been studied by many groups.^{28,38,40} Attempts to understand these systems were mostly focused on the wetting of a low density isotropic array of pillars since for such a texture the advancing and even receding angles are outstandingly large.³⁹ The surface with holes does not have this property because of a much higher solid fraction, which inevitably makes the contact angle smaller. The same remark concerns the case of stripes, which is also different because it introduces some anisotropy in wetting and in the hysteresis of the contact angle.^{41,42} However, despite an increasing body of publications on wetting of anisotropic,³⁰ complex⁴³ and hierarchical surfaces, the quantitative understanding of these systems is still at its infancy.

The important property of superhydrophobic surfaces is a contact angle hysteresis,⁴⁴ which is due to the roughness or heterogeneity of the interface and the elasticity of a contact line.^{3,45} The hysteresis and pinning are huge at the Wenzel state, which causes a strong adhesion of the drop to such a surface. However, the hysteresis is normally low at the Cassie state, and this allows one a remarkable mobility of the drop, which renders surfaces self-cleaning, and causes droplets to roll (rather than slide) under gravity and rebound (rather than spread) upon impact.^{9,46,47} The reduction in contact angle hysteresis can dramatically improve droplet mobility and mixing following droplet coalescence in droplet-based, so-called digital microfluidics.⁴⁸ However, a moderate hysteresis of the contact angles at the directional Cassie surfaces could also be employed in microfluidic devices since it allows one to deflect, sort and capture drops.⁴⁹

Finally, note that even when the Cassie-to-Wenzel transition takes place, it is not clear how to induce the opposite Wenzel-to-Cassie route, and the transition between the two states is strongly hysteretic. Some preliminary ideas, such as heating or surface vibration⁵⁰ and electrowetting⁵¹ have been proposed. Recent ideas include a gas-restoration mechanism on surfaces with multiple length scales.⁵² However, more work in this area will be needed.

Shift of focus: transport phenomena

During the last few years it was well recognized that the unique properties of superhydrophobic materials can significantly impact transport phenomena so that the field has expanded beyond wetting. As we mentioned above, already the observation of an unusual mobility of a drop at superhydrophobic surfaces suggested some microfluidic applications,⁴⁹ and it also raised the stimulating question of a possible effective hydrodynamic slip.¹⁰ A liquid flowing on a hydrophilic solid does not slip at the interface between both phases, but a slip length b (the distance within the solid at which the flow profile extrapolates to zero) might exist if the solid is hydrophobic.^{53–55} For hydrophobic smooth and

homogeneous surfaces, b can be of the order of tens of nanometers,^{56–58} but not much more. This effect can be dramatically amplified if the hydrophobic solid is rough, provided that air is trapped in the textures.^{59,60} Therefore, one could potentially benefit from such a slip in various lab-on-a-chip applications,²¹ fuel transport, cooling of electronic chips, *etc.* This related to reduced drag ability, new topic of interest appears to be a rewarding one for the field as a whole. Below we describe these new opportunities.

In response to the challenge of building superhydrophobic surfaces for microfluidics, research efforts have mainly focused on the design of new types of patterned materials to manipulate flows and on the characterization of their friction properties. New investigations required new methods to quantify the effective properties of superhydrophobic surfaces since the traditional approach based on characterizing superhydrophobic materials by using solely their contact angle cannot provide a physical insight into transport phenomena. Instead, the drag reduction can be quantified by an effective slip length of the heterogeneous Cassie surface, which refers to a situation where slippage at a complex heterogeneous surface is evaluated by flow averaging over the length scale of the experimental configuration^{18,21,61,62} (see Figure 3). Straightforward calculations^{53,63} suggest that a lubricating gas film of a thickness h of viscosity η_g (which is about 50 times smaller than the viscosity of a liquid, η) leads to the apparent local slip

$$b = h \left(\frac{\eta}{\eta_g} - 1 \right) \approx h \frac{\eta}{\eta_g}. \quad (6)$$

Therefore, slip lengths up to hundreds of μm may be then obtained over a gas layer stabilized with a rough texture. However, the composite nature of the interface requires regions of lower slip (or no slip) in direct contact with the liquid, so the effective slip length of the superhydrophobic surface is reduced.

A significant progress has been made during past years in the quantitative understanding of an effective slippage past superhydrophobic surfaces. In contrast to wetting studies, the major focus was on surfaces with directional patterns, such as the arrays of parallel superhydrophobic grooves that generate anisotropic effective slip in the Cassie regime. The hydrodynamic slip is different along and perpendicular to the stripes. Axial motion is preferred, and such designs are appropriate when liquid must be

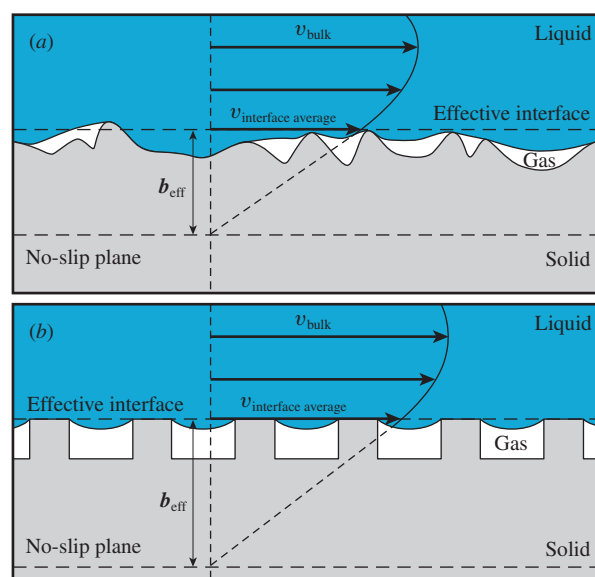


Figure 3 Schematic diagram of velocity profiles and effective slip lengths, b_{eff} , near (a) randomly rough and (b) periodic superhydrophobic surfaces. Disordered surfaces display a broad spectrum of scales. Instead, periodic surfaces are typically characterized by a characteristic length of a texture, L , local slip at the gas area, b , and a fraction of the liquid–solid interface, φ_S .

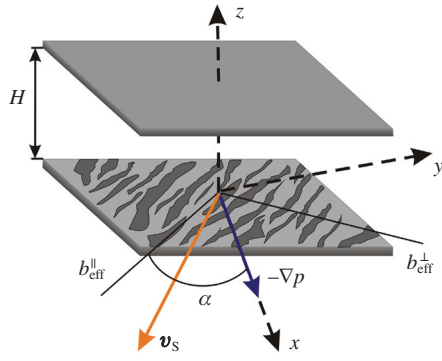


Figure 4 Sketch of a flat channel of thickness H with notation for directions along the plates. One wall represents an anisotropic superhydrophobic texture (adapted from ref. 18). The driving force, here a uniform pressure gradient, $-\nabla p$, produces an effective slip velocity, \mathbf{v}_s , in a different direction.

guided. The flow anisotropy is characterized by the second-rank effective slip tensor, $\mathbf{b}_{\text{eff}} \equiv \{b_{ij}^{\text{eff}}\}$, and is represented by a symmetric, positive definite 2×2 matrix diagonalized by a rotation

$$\mathbf{b}_{\text{eff}} = S_{\alpha} \begin{pmatrix} b_{\text{eff}}^{\parallel} & 0 \\ 0 & b_{\text{eff}}^{\perp} \end{pmatrix} S_{\alpha}^{-1}, \quad S_{\alpha} = \begin{pmatrix} \cos \alpha & \sin \alpha \\ -\sin \alpha & \cos \alpha \end{pmatrix}. \quad (7)$$

Therefore, the flow along any direction of the anisotropic surface can be determined, once the eigenvalues of the effective slip tensor are found from the known spatially nonuniform scalar slip. For all anisotropic surfaces, the eigenvalues $b_{\text{eff}}^{\parallel}$ and b_{eff}^{\perp} of the slip-length tensor correspond to the fastest (greatest forward slip) and slowest (least forward slip) orthogonal directions⁶¹ (see Figure 4). In the general case of any direction α , this means that the flow past such surfaces becomes misaligned with the driving force, which is due to the generation of a secondary (transverse) flow.^{18,64}

The quantitative understanding of liquid slippage even in case of a single anisotropic superhydrophobic surface (where $H \gg L$) is still challenging. The problem was tackled theoretically,^{36,65–67} and several numerical approaches have also been proposed either at the molecular scale, using molecular dynamics,⁶⁸ or at larger mesoscopic scales using finite element methods,⁶⁹ lattice Boltzmann^{70,71} or dissipative particle dynamics⁷² simulations. Recent work suggested that for any anisotropic surface with arbitrary scalar slip $b(y)$ varying in only one direction, the transverse component of the effective slip-length tensor is equal to a half of the longitudinal one with a two times larger local slip⁷³

$$b_{\text{eff}}^{\perp}[b(y)/L] = \frac{b_{\text{eff}}^{\parallel}[b(2y)/L]}{2}. \quad (8)$$

This result opened the possibility of solving a broad class of hydrodynamic problems for one-dimensional single textured surfaces. For patterns composed of no-slip and partial slip stripes (*i.e.*, flat liquid–gas interface), $b_{\text{eff}}^{\parallel}$ is⁶⁵

$$b_{\text{eff}}^{\parallel} \approx \frac{L}{\pi} \frac{\ln\{\sec[\pi(1 - \varphi_S)/2]\}}{1 + (L/\pi b) \ln\{\sec[\pi(1 - \varphi_S)/2] + \tan[\pi(1 - \varphi_S)/2]\}}. \quad (9)$$

For a flow in a transverse configuration, b_{eff}^{\perp} , the result⁶⁵ can be easily found from equation (9) by applying equation (8). The largest anisotropy of the flow is expected at the limit of $b \gg L$ (which was shown to be mathematically equivalent to a perfect slip, $b \rightarrow \infty$),⁶⁶ *i.e.*, when the eigenvalues of the slip-length tensor are maximal. However, the flow becomes isotropic in the opposite limit of $b \ll L$, suggesting that the interplay of different length scales can be used to impact flow properties even qualitatively. For example, in the situation of a large $b_{\text{eff}}^{\parallel} - b_{\text{eff}}^{\perp}$ one can generate a secondary flow transverse to the direction of an applied force in the vicinity of a superhydrophobic wall by making the velocity profile twisted.¹⁸ Therefore, superhydrophobic surfaces may find applications in passive microfluidic mixing⁷⁴ or separation of particles and/or biomolecules.

However, most solids are isotropic, that is, without a preferred direction. This situation is more complicated than that considered above. Nevertheless, the simplest scaling expressions^{55,75} have been proposed for the geometry of pillars (in the idealized case of perfect slip, $b \rightarrow \infty$, at the gas sectors) by predicting $b_{\text{eff}} \propto L/(\pi\varphi_S^{1/2})$, which suggests that in the limit of $\varphi_S \rightarrow 0$ the array of pillars should give a larger effective slip than longitudinal stripes. Recent approximate analysis⁷⁶ and semi-analytical results⁷⁷ justified this scaling dependence. Note that, recently, attempts have also been made to evaluate effective slips for isotropic mesh-like⁷⁸ and fractal⁷⁹ surfaces. However, our fundamental understanding of flow past isotropic surfaces has just begun.

A conclusion from the above analysis is that the effective slip is maximized by reducing the solid–liquid area fraction φ_S and increasing the local slip at the gas sectors, and the role of the texture geometry is essential. Several experimental studies have been conducted to verify these theoretical predictions for both random isotropic⁸⁰ and periodic surfaces.^{81–83} In most of the studies, there has been qualitative (or nearly quantitative) agreement with the theoretical expectations, but the measured slip was only about a few micrometers. This could indicate that the current analytical models of superhydrophobic slip neglect the meniscus curvature, which introduces an additional dissipation mechanism.^{67,75,84} These relatively low values of an effective slip are also partly due to a relatively large liquid–solid area fraction. Since at low φ_S the Cassie state is metastable, it is difficult to obtain a giant effective slip with simple patterns. To increase the stability of the gas phase, it has been suggested to use hierarchical patterns.^{2,79,85} Such complex hierarchical patterns, which combine roughness on micro- and nanoscales, are very common in nature.¹⁶ It is reasonable to expect that, in synthetic biomimetic surfaces, the microtexture would provide a large slip, while the presence of a secondary nanotexture could improve the stability of the Cassie state. Indeed, the presence of a secondary texture was shown to decrease the slip length.^{86,87} We remark that a slip in the hundreds of micron range was reported for such surfaces by using the rheological method. Note that for all types of textures the results obtained with the rheometry technique are far larger than measured by a velocimetry flow profiling, so that would require further verification and theoretical understanding.

We remind that the above results apply only for a single surface. If the flow is conducted in a channel with two confining surfaces separated by a distance $H \leq L$, the eigenvalues of the slip-length tensor become dependent on H ,^{62,70} which reflects the fact that an effective slip is not a characteristic of the superhydrophobic interface solely, but it may depend on the flow configuration.^{18,55} In the general case of an arbitrary channel thickness, the problem can only be treated semi-analytically or numerically.^{70,72} However, some general principles to maximize or minimize the effective slip can be suggested in the lubrication limit, $H \ll L$ (see Figure 5).^{62,88} Among all possible textures, parallel stripes attain the largest (or smallest) possible slip in a thin channel for a parallel (or perpendicular) orientation with respect to the mean flow. Bounds for isotropic textures are tighter, and the upper (lowest) bounds for effective slip can be attained for a special Hashin-Strikman pattern. However, the fractal geometry is not necessary since periodic honeycomb-like structures can also attend the bounds. Finally, in the particular case of a medium that is invariant by a rotation followed by a $\pi/2$ phase interchange (chessboards, *etc.*) the effective slip is¹⁸

$$b_{\text{eff}} = \frac{3H}{4 - \sqrt{1 + 3b/(H + b)}} - H. \quad (10)$$

Note that in the limit $H \gg b$ for all textures the effective slip coincides with surface average. If $H \ll b$, $b_{\text{eff}} \propto (1 - \varphi_S)/\varphi_S$ for all patterns. This suggests that the key parameter determining effective

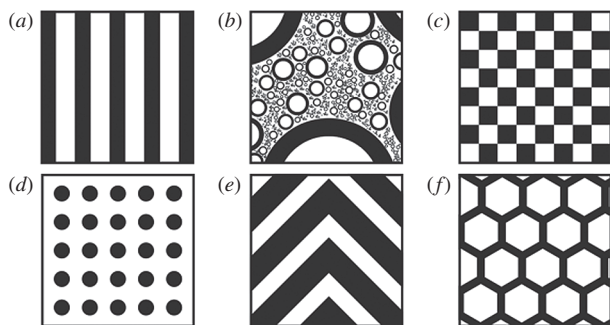


Figure 5 Special textures arising in theory for a thin channel:^{62,64,88} (a) stripes, which attain the Wiener bounds of the maximal and minimal effective slip, if oriented parallel or perpendicular to the pressure gradient, respectively; (b) the Hashin–Shtrikman fractal pattern of nested circles, which attains the maximal/minimal slip among all isotropic textures (patches should fill up the whole space, but their number is limited here for clarity); (c) the chessboard texture, whose effective slip follows from the phase-interchange theorem; (d) circular pillars; (e) the parquet texture for mixing/separation and (f) honeycomb texture.

slip in a thin channel is the solid area fraction, which should be minimized. If it is very small, $\varphi_S \rightarrow 0$, such a thin channel can even produce a kind of superfluidity with a plug-like flow.⁶²

A straightforward implication of a superhydrophobic slip in a thin channel would be the generation of a very strong transverse flow, which is much more efficient than that in a thick channel.¹⁸ A thin channel situation is also more appropriate since the largest transverse flow is generated at intermediate values of solid fractions, namely, at $\varphi_S = 0.5$, where the effective (forward) slip is relatively small, but the Cassie state is typically stable.^{64,72} An important conclusion from this result is that the surface texture which optimizes a transverse flow can significantly differ from the optimizing slip.

Hydrodynamic drag in a thin gap have been recently measured with the surface force apparatus,⁸⁹ and atomic force microscopy.⁹⁰ The extracted slip length from the fitting of experimental data was of the order of 100 nm, which is only slightly larger than at smooth hydrophobic solid and much smaller than in case of a single superhydrophobic interface. This is qualitatively consistent with the theoretical predictions on a dependency of slip on the height of the channel.⁷⁰ However, in their analysis authors make assumptions of a constant isotropic, homogeneous, and independent of distance slip that are not generally valid for a heterogeneous superhydrophobic surface as discussed above. We suggest that further analysis of these measurements or similar measurements with other textures should employ recent analysis that takes these effects into account.⁹¹

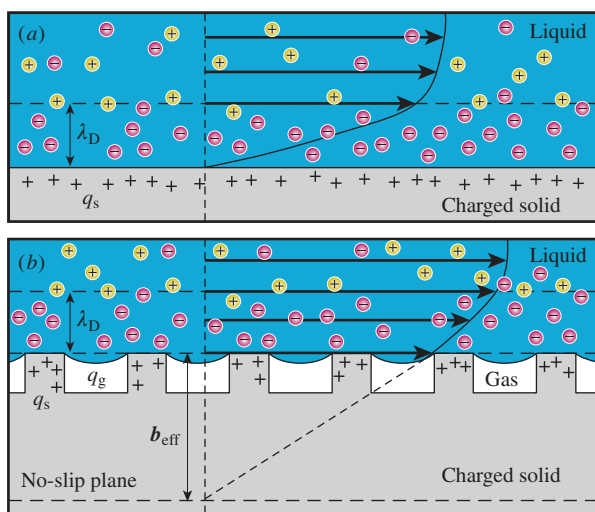


Figure 6 Electro-osmotic flow on (a) hydrophilic and (b) superhydrophobic surfaces. The tangential electric field E is directed to the left.

An alternative method to generate a fluid flow in microfluidics is electro-osmosis, *i.e.*, flow generation by an electric field (Figure 6). The fluid outside of the electric double layer (of a thickness of the order of the Debye length, λ_D) moves as a plug, which has many advantages as compared with conventional pressure-driven flows.^{21,92} As discussed earlier,^{93–95} electro-osmotic flow can be significantly amplified by an effective superhydrophobic slip provided the gas–liquid interface is charged, which is not an unrealistic assumption.⁹⁶ For example, for uniformly charged ($q_g = q_s = q_0$) anisotropic superhydrophobic surfaces (in the limit $b \rightarrow \infty$), the electroosmotic velocity reads

$$\mathbf{u} = -\frac{Eq_0\lambda_D}{\eta} \left(\mathbf{I} + \frac{\mathbf{b}_{\text{eff}}}{\lambda_D} \right), \quad (11)$$

where \mathbf{I} is the unit tensor. The flow is truly anisotropic, and it can exhibit a large, possibly one or two order of magnitude enhancement even at relatively large φ_S . An interesting scenario is expected for oppositely charged gas and solid sectors ($q_g = -q_s = -q_0$), which leads to

$$\mathbf{u} = -\frac{Eq_0\lambda_D}{\eta} \left(\mathbf{I} - \frac{\mathbf{b}_{\text{eff}}}{\lambda_D} \right), \quad (12)$$

by suggesting a very reach behaviour. For example, an inhomogeneous surface charge can induce a flow along and opposite to the field, depending on φ_S . Another striking result is that an electroneutral superhydrophobic surface can generate an extremely large electro-osmotic slip.⁹⁴ Strong enhancement of transport on superhydrophobic surfaces was also predicted for diffusio-osmosis – the motion of a fluid induced by a solute gradient.⁹⁷ These effects remain to be proven experimentally, and they could be very important in the context of energy conversion devices and many other applications.

Fabrication of superhydrophobic surfaces: design, materials and methods

There are now enough methods of fabrication of superhydrophobic surfaces for various, mostly non-wetting applications. Below we briefly summarize some of them. Here, we do not intend to provide a comprehensive report on available methods for the fabrication of superhydrophobic surfaces, which can be found in reviews,^{14–16,98} but rather summarize important recent developments relevant for microfluidics applications.

Most experimental methods allow one to produce randomly rough superhydrophobic surfaces. They include sol-gel based methods, chemical deposition, sublimation, controlled polymerization, self-assembly of nanorods and nanotubes on the surfaces, electrochemical methods *etc.* (Figure 7).^{7,11,14} Since the control of φ_S is impossible with randomly rough surfaces, these surfaces are often (but not always) wetted in the Wenzel regime.

Electrochemical methods include electrochemical deposition,^{100,101} electrochemical polymerization,^{102,103} electrospinning,^{30,104} reactions in galvanic cells,¹⁰⁵ *etc.* These methods are usually used for the fabrication of rough metal surfaces. The roughness of the surface is controlled by the duration of treatment and the applied voltage. The advantage of the electrochemical methods is weak dependence on the properties of substrates. These can be oxides, some metals or different types of polymer matrices, for instance, based on polyelectrolytes.¹⁰⁰ The methods allow one to fabricate the surfaces with different morphology: they can consist of spheres, clusters, whiskers or rods of different size and shape.^{30,104}

The sol-gel methods^{99,106} based on a sol-gel transition are often used for the preparation of oxide surfaces or their organic derivatives. The hydrolysis and condensation steps allow one to control the foam formations to get the surface of the required roughness. The alcoholates of various metals (Zn, Al and Ti) or silicon are used as precursors.^{99,107–109}

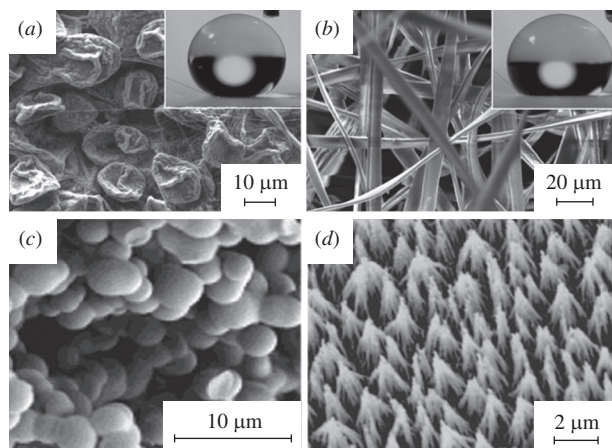


Figure 7 Randomly rough superhydrophobic surfaces: (a) and (b) polymer-based coatings obtained by electrospinning (reprinted with permission from ref. 30, © 2008, by The National Academy of Sciences of the USA); (c) gold-coated foams obtained *via* the sol-gel processing of methyltriethoxysilane (reprinted with permission from ref. 99, © 2003, by American Chemical Society); and (d) carbon nanotubes forest after functionalization with thiols (reprinted with permission from ref. 80, © 2006, by The American Physical Society).

Chemical vapor deposition is one of the most efficient ways to produce surfaces with random roughness or partially ordered nanotube/nanorod arrays. Surfaces are made of different polymers, such as polymethylsilsequioxane,¹¹⁰ silicon elastomers⁴ or inorganic compounds (carbon nanotubes,⁸⁰ metals or oxides^{111–113}). Surface properties are controlled by the gas pressure and temperature of substrates. To improve the properties of surfaces, the method is often used in combination with plasma treatment (so-called plasma assisted chemical vapor deposition),¹¹² or aerosol producing (aerosol assisted chemical vapor deposition).⁴ This post-treatment allows one to control the texture parameters. The related method of sublimation is used for the fabrication of randomly rough surfaces prepared by the sublimation of the volatile precursors (usually acetylacetonates) of metal oxides.¹⁰⁰

Randomly rough surfaces can also be obtained by hydrothermal methods,¹¹⁴ layer-by-layer deposition,¹⁰¹ femtosecond laser irradiation¹¹⁵ *etc.* Recently the graphene-based materials have also been shown¹¹⁶ to possess superhydrophobic properties.

Methods of fabrication of textured surfaces with well-defined topology are based on etching the surface through the mask pre-set digitally (in chemical and electron etching methods), or on replication of the surface with existing texture (lithography, 2D photonic crystals and anodized aluminum oxide).

In template-based methods, membranes with an ordered array of one-dimensional pores with a well-defined size are normally used. As a matrix, one can use anodized aluminum oxide.¹¹⁷ Poly-

mers (such as PVA and PAN) can be used as precursors, which crystallize in the pores. These methods have some disadvantages, so that we focus on more advanced lithography techniques below.

Lithography methods (Figure 8) are based on the use of well-defined templates, so that the texture is accurately set in advance (in the program controlling the electron etching process, printed mask, rigid template replicable onto another material *etc.*). Such types of lithography as electron and ion etching, soft lithography and photolithography are already very well-developed and widely used. Beside there are some novel methods of lithography based on imprint processes and a combination of several types of lithography as we discuss below.

The electron-beam etching lithography uses an electron beam, which is scanning the surface of the electron resist creating the template texture set digitally (with a nanometer resolution). Usually, such (expensive!) surfaces are used as masters to produce other surfaces (by using other types of lithography).

The deep reactive ion etching uses reactive plasma, which etches the chemically unprotected areas of a material. The protecting chemical coating is added through the mask and is not sensitive to gas plasma. The type and amount of gas depends on the material to etch. For example, silicon surfaces require SF₆ plasma. This method is cheaper and easier, but it is also used to fabricate masters for other types of lithography.

Photolithography exploits photosensitive polymers that cover substrates and are irradiated (usually by UV light) through the previously printed mask. The UV-opaque masks could be produced with a submicron resolution. The photoresist can cross-link under radiation (so-called positive photoresist) or, oppositely, it can dissolve during the exposure (negative photoresist). The not cross-linked part of the polymer can be removed after the exposure.

Soft lithography is currently the most popular method since it is simple, cheap and flexible.^{118,119} The method uses masters fabricated by photolithography, electron or reactive ion lithography. These masters are replicated on an elastic PDMS polymer. Cross-linking leads to the formation of an elastic material, which replicates the texture of the master. PDMS with its excellent optical transparency, low toxicity and high permeability to oxygen and carbon dioxide is a material suitable for the fabrication of microchannels to manipulate with biological cells, and microfluidic PDMS systems have already found applications in cell biology.²³ However, PDMS has some disadvantages when microfluidic systems are used for chemical synthesis (especially in organic and medicinal chemistry) since it dissolves, or swells in common organic solvents.¹²⁰ The use of polymers other than PDMS can solve this problem and allows reactions to proceed at high temperature and pressure, but the fabrication could be more difficult.

The same remarks concern the use of glass materials, which can be obtained by nanoimprint lithography. This technique is

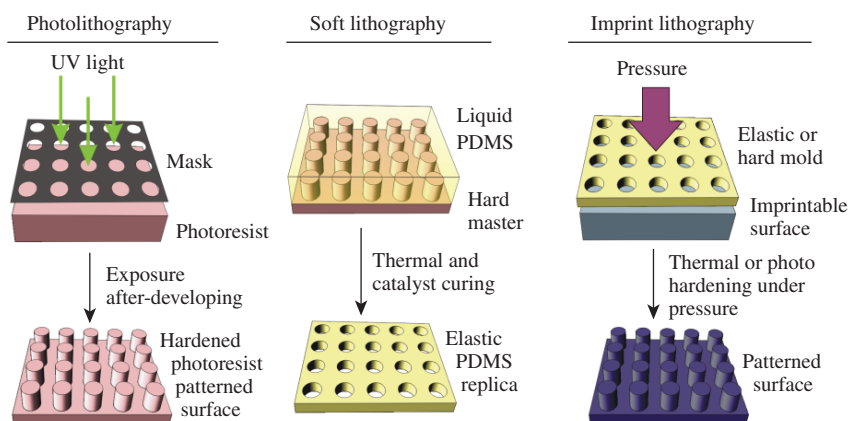


Figure 8 Schematics of lithographic techniques as a sequence of stages: the optical lithography on photoresist; the soft lithography using the photolithographed pattern as a master; imprint lithography using PDMS replica as a mold.

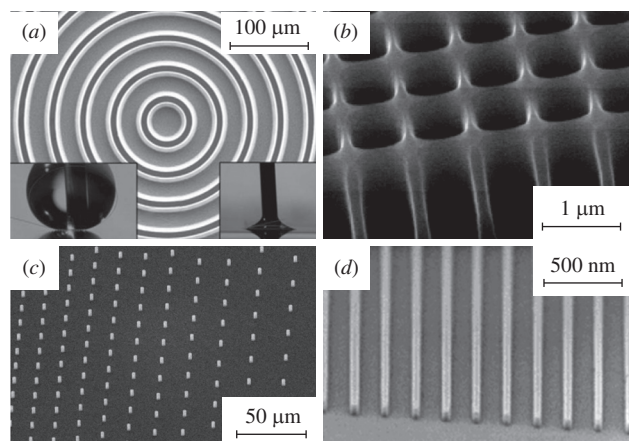


Figure 9 Different types of superhydrophobic textured surfaces for microfluidic applications obtained by lithographic methods: (a) concentric circular striped texture (reprinted with permission from ref. 41, © 2009, by Elsevier Inc.) so that the grates are parallel to a liquid flow in the rheometer system; (b) circular holes used in the surface force apparatus experiment (reprinted with permission from ref. 89, © 2008, by The American Physical Society); (c) the array of pillars with gradient of ϕ_s , (reprinted with permission from ref. 127, © 2009, by EPL Association) which can be used to generate a locomotion of the drop in a droplet-based microfluidics; (d) array of parallel nanometric stripes (reprinted with permission from ref. 128, © 2005, by American Chemical Society).

already exploited in industry for the production of compact discs, diffraction gratings *etc.*, and the resolution of this technique has already reached 10 nm. Resist materials are normally thermoplastic polymers^{121–123} or polymeric UV resists.¹²³ Another type of resists is the so-called sol-gel resist^{3,124–126} that makes it possible to fabricate oxide and oxide-organic surfaces. This method represents an important step forward, and it can be used to texture large areas, which could be important for high-value applications of microfluidic systems.

In general, the modern lithography methods allow one to fabricate various complex textures (see Figure 9), which could be useful in superhydrophobic microfluidics.

Finally, note that most of the textures produced by modern fabrication methods are not hydrophobic, and they require some chemical treatment (hydrophobization) to become superhydrophobic. The hydrophobization can be performed by physical or chemical adsorption (Figure 10). The latter can be carried out in a water or gas phase using (depending on the material of the texture) alkanethiols derivatives,¹²⁹ silane-based organic compounds, fatty acids¹³⁰ *etc.* The bounding group of the hydrophobizer should be chosen according to the material of the patterned surface: usually it is thiol for the metallic surfaces and silane chloride (or other easily hydrolyzed silane derivatives) for silica and silica based polymers (as PDMS) and metal oxides.

Conclusions and future directions

In this short review we have tried to discuss the new opportunities in research on superhydrophobic materials, related to greatly enhanced transport properties, which could be very important for manipulations of liquids in microfluidic devices. In particular, advances in lithography to pattern substrates have raised several questions in the modeling of liquid motions over these surfaces and led to the concept of the effective tensorial slip past superhydrophobic surfaces with trapped gas. Such surfaces have the potential to influence microfluidics (or to extend microfluidic systems to nanofluidics), by generating very fast and well controlled forward and transverse flows in smaller devices. But the field is still at an early stage of development, and would require further development, both at the level of basic science and technologies. Many problems must still be addressed, and many challenges remain. For example, there is quantitative discrepancy

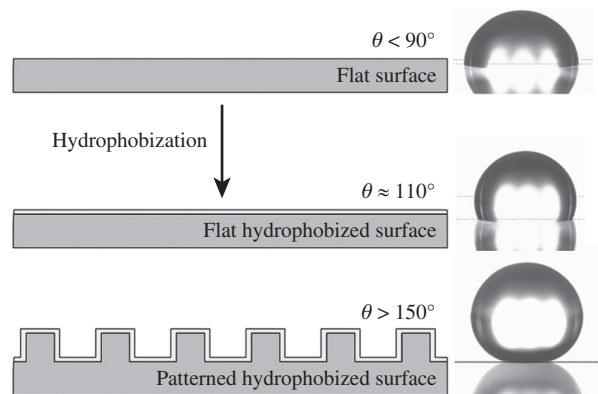


Figure 10 Contact angle evolution after the hydrophobization of flat and patterned surfaces. Hydrophobizer: $\text{SiCl}_3\text{-C}_n\text{F}_{2n-1}$; fatty acids *etc.*

between theory and experiment, which has to be understood. There are many opportunities to design new experiments and to develop improved theoretical models for electro-osmosis near superhydrophobic surfaces. Very promising directions are certainly diffusio-osmosis and thermo-osmosis, which could lead to a giant amplification of flow in microchannels, even if the liquid–gas interface is uncharged. The solutions to these problems will require new theoretical and experimental approaches, and we expect a significant expansion into this very interesting area of research.

We are grateful to E. S. Asmolov, E. Barthel, M. Z. Bazant, A. V. Belyaev, F. Feuillebois, J. Teisseire and D. Quere for many stimulating discussions. This work was supported by the Russian Academy of Sciences (priority programme ‘Assembly and Investigation of Macromolecular Structures of New Generations’).

References

- 1 C. Neinhuis and W. Barthlott, *Ann. Bot.*, 1997, **79**, 667.
- 2 T. Onda, S. Shibuichi, N. Satoh and K. Tsujii, *Langmuir*, 1996, **12**, 2125.
- 3 A. L. Dubov, J. Teisseire and E. Barthel, *EPL*, 2012, **97**, 26003.
- 4 C. R. Crick and I. P. Parkin, *J. Mater. Chem.*, 2009, **19**, 1074.
- 5 R. N. Wenzel, *Ind. Eng. Chem.*, 1936, **28**, 988.
- 6 A. B. D. Cassie and S. Baxter, *Trans. Faraday Soc.*, 1944, **40**, 546.
- 7 N. J. Shirtcliffe, G. McHale, S. Atherton and M. I. Newton, *Adv. Colloid Interface Sci.*, 2010, **161**, 124.
- 8 M. Nosonovsky and B. Bhushan, *Curr. Opin. Colloid Interface Sci.*, 2009, **14**, 270.
- 9 D. Quere, *Rep. Prog. Phys.*, 2005, **68**, 2495.
- 10 M. Callies and D. Quere, *Soft Matter*, 2005, **1**, 55.
- 11 B. Bhushan and Y. C. Jung, *Prog. Mater. Sci.*, 2011, **56**, 1.
- 12 S. Herminghaus, *Europhys. Lett.*, 2000, **52**, 165.
- 13 O. Sato, S. Kubo and Z. Z. Gu, *Acc. Chem. Res.*, 2009, **42**, 1.
- 14 X. M. Li, D. Reinhoudt and M. Crego-Calama, *Chem. Soc. Rev.*, 2007, **36**, 1350.
- 15 F. Xia and L. Jiang, *Adv. Mater.*, 2008, **20**, 2842.
- 16 Z. Guo, W. Liu and B. L. Su, *J. Colloid Interface Sci.*, 2011, **353**, 333.
- 17 L. Bocquet and E. Lauga, *Nat. Mater.*, 2011, **10**, 334.
- 18 O. I. Vinogradova and A. V. Belyaev, *J. Phys. Condens. Matter*, 2011, **23**, 184104.
- 19 G. McHale, M. I. Newton and N. J. Shirtcliffe, *Soft Matter*, 2010, **6**, 714.
- 20 M. Reyssat, D. Richard, C. Clanet and D. Quere, *Faraday Discuss.*, 2010, **146**, 19.
- 21 H. A. Stone, A. D. Stroock and A. Ajdari, *Annu. Rev. Fluid Mechanics*, 2004, **36**, 381.
- 22 D. Quere, *Annu. Rev. Mater. Res.*, 2008, **38**, 71.
- 23 G. M. Whitesides, *Nature*, 2006, **442**, 368.
- 24 A. V. Belyaev and O. I. Vinogradova, *Soft Matter*, 2010, **6**, 4563.
- 25 N. A. Patankar, *Langmuir*, 2004, **20**, 7097.
- 26 A. Lafuma and D. Quere, *Nat. Mater.*, 2003, **2**, 457.
- 27 A. Marmur, *Langmuir*, 2003, **19**, 8343.
- 28 M. Reyssat, J. M. Yeomans and D. Quere, *EPL*, 2008, **81**, 26006.
- 29 C. Ishino, K. Okumura and D. Quere, *Europhys. Lett.*, 2004, **68**, 419.
- 30 A. Tuteja, W. Choi, J. M. Mabry, G. H. McKinley and R. E. Cohen, *Proc. Natl. Acad. Sci. USA*, 2008, **105**, 18200.
- 31 C. W. Extrand, *Langmuir*, 2002, **18**, 7991.
- 32 N. Verplanck, Y. Coffinier, V. Thomy and R. Boukherroub, *Nanoscale Res. Lett.*, 2007, **2**, 577.
- 33 J. Heikenfeld and M. Dhindsa, *J. Adhesion Sci. Technol.*, 2008, **22**, 319.

- 34 N. T. Nguyen, G. P. Zhu, Y. C. Chua, V. N. Phan and S. H. Tan, *Langmuir*, 2010, **26**, 12553.
- 35 A. Dupuis and J. M. Yeomans, *Langmuir*, 2005, **21**, 2624.
- 36 C. Cottin-Bizonne, C. Barentin, E. Charlaix, L. Bocquet and J. L. Barrat, *Eur. Phys. J. E*, 2004, **15**, 427.
- 37 A. Tuteja, W. Choi, M. L. Ma, J. M. Mabry, S. A. Mazzella, G. C. Rutledge, G. H. McKinley and R. E. Cohen, *Science*, 2007, **318**, 1618.
- 38 S. Moulinet and D. Bartolo, *Eur. Phys. J. E*, 2007, **24**, 251.
- 39 J. Bico, C. Marzolin and D. Quere, *Epl*, 1999, **47**, 220.
- 40 C. Pirat, M. Sbragaglia, A. M. Peters, B. M. Borkent, R. G. H. Lammertink, M. Wessling and D. Lohse, *Epl*, 2008, **81**, 66002.
- 41 W. Choi, A. Tuteja, J. M. Mabry, R. E. Cohen and G. H. McKinley, *J. Colloid Interface Sci.*, 2009, **339**, 208.
- 42 O. Bliznyuk, V. Veligura, E. S. Kooij, H. J. W. Zandvliet and B. Poelsma, *Phys. Rev. E*, 2011, **83**, 041607.
- 43 A. M. Peters, C. Pirat, M. Sbragaglia, B. M. Borkent, M. Wessling, D. Lohse and R. G. H. Lammertink, *Eur. Phys. J. E*, 2009, **29**, 391.
- 44 J. F. Joanny and P. G. de Gennes, *J. Chem. Phys.*, 1984, **81**, 552.
- 45 M. Reyssat and D. Quere, *J. Phys. Chem. B*, 2009, **113**, 3906.
- 46 G. McHale, N. J. Shirtcliffe and M. I. Newton, *Langmuir*, 2004, **20**, 10146.
- 47 D. Oner and T. J. McCarthy, *Langmuir*, 2000, **16**, 7777.
- 48 J. P. Rothstein, *Annu. Rev. Fluid Mechanics*, 2010, **42**, 89.
- 49 M. A. Nilsson and J. P. Rothstein, *Phys. Fluids*, 2012, **24**, 062001.
- 50 E. Bormashenko, R. Pogreb, G. Whyman, Y. Bormashenko and M. Erlich, *Appl. Phys. Lett.*, 2007, **90**, 201917.
- 51 G. Manukyan, J. M. Oh, D. van den Ende, R. G. H. Lammertink and F. Mugele, *Phys. Rev. Lett.*, 2011, **106**, 014501.
- 52 C. Lee and C. J. Kim, *Langmuir*, 2009, **25**, 12812.
- 53 O. I. Vinogradova, *Langmuir*, 1995, **11**, 2213.
- 54 O. I. Vinogradova, *Int. J. Miner. Process.*, 1999, **56**, 31.
- 55 L. Bocquet and J. L. Barrat, *Soft Matter*, 2007, **3**, 685.
- 56 O. I. Vinogradova and G. E. Yakubov, *Langmuir*, 2003, **19**, 1227.
- 57 O. I. Vinogradova, K. Koynov, A. Best and F. Feuillebois, *Phys. Rev. Lett.*, 2009, **102**, 118302.
- 58 C. Cottin-Bizonne, B. Cross, A. Steinberger and E. Charlaix, *Phys. Rev. Lett.*, 2005, **94**, 056102.
- 59 O. I. Vinogradova, N. F. Bunkin, N. V. Churaev, O. A. Kiseleva, A. V. Lobeyev and B. W. Ninham, *J. Colloid Interface Sci.*, 1995, **173**, 443.
- 60 C. Cottin-Bizonne, J. L. Barrat, L. Bocquet and E. Charlaix, *Nat. Mater.*, 2003, **2**, 237.
- 61 M. Z. Bazant and O. I. Vinogradova, *J. Fluid Mechanics*, 2008, **613**, 125.
- 62 F. Feuillebois, M. Z. Bazant and O. I. Vinogradova, *Phys. Rev. Lett.*, 2009, **102**, 026001.
- 63 D. Andrienko, B. Dunweg and O. I. Vinogradova, *J. Chem. Phys.*, 2003, **119**, 13106.
- 64 F. Feuillebois, M. Z. Bazant and O. I. Vinogradova, *Phys. Rev. E*, 2010, **82**, 055301(R).
- 65 A. V. Belyaev and O. I. Vinogradova, *J. Fluid Mechanics*, 2010, **652**, 489.
- 66 E. Lauga and H. A. Stone, *J. Fluid Mechanics*, 2003, **489**, 55.
- 67 M. Sbragaglia and A. Prosperetti, *Phys. Fluids*, 2007, **19**, 043603.
- 68 N. V. Priezjev, *J. Chem. Phys.*, 2011, **135**, 204704.
- 69 N. V. Priezjev, A. A. Darhuber and S. M. Troian, *Phys. Rev. E*, 2005, **71**, 041608.
- 70 S. Schmieschek, A. V. Belyaev, J. Harting and O. I. Vinogradova, *Phys. Rev. E*, 2012, **85**, 016324.
- 71 J. Hyväluoma, C. Kunert and J. Harting, *J. Phys. Condens. Matter*, 2011, **23**, 184106.
- 72 J. J. Zhou, A. V. Belyaev, F. Schmid and O. I. Vinogradova, *J. Chem. Phys.*, 2012, **136**, 194706.
- 73 E. S. Asmolov and O. I. Vinogradova, *J. Fluid Mechanics*, 2012, **706**, 108.
- 74 A. D. Stroock, S. K. W. Dertinger, A. Ajdari, I. Mezic, H. A. Stone and G. M. Whitesides, *Science*, 2002, **295**, 647.
- 75 C. Ybert, C. Barentin, C. Cottin-Bizonne, P. Joseph and L. Bocquet, *Phys. Fluids*, 2007, **19**, 123601.
- 76 A. M. J. Davis and E. Lauga, *J. Fluid Mechanics*, 2010, **661**, 402.
- 77 C. O. Ng and C. Y. Wang, *Microfluid. Nanofluid.*, 2010, **8**, 361.
- 78 A. M. J. Davis and E. Lauga, *Phys. Fluids*, 2009, **21**, 113101.
- 79 C. Cottin-Bizonne, C. Barentin and L. Bocquet, *Phys. Fluids*, 2012, **24**, 012001.
- 80 P. Joseph, C. Cottin-Bizonne, J. M. Benoit, C. Ybert, C. Journet, P. Tabeling and L. Bocquet, *Phys. Rev. Lett.*, 2006, **97**, 156104.
- 81 J. Ou, B. Perot and J. P. Rothstein, *Phys. Fluids*, 2004, **16**, 4635.
- 82 P. Tsai, A. M. Peters, C. Pirat, M. Wessling, R. G. H. Lammertink and D. Lohse, *Phys. Fluids*, 2009, **21**, 112002.
- 83 C. H. Choi, U. Ulmanella, J. Kim, S. M. Ho and C. J. Kim, *Phys. Fluids*, 2006, **18**, 097105.
- 84 J. Hyväluoma and J. Harting, *Phys. Rev. Lett.*, 2008, **100**, 246001.
- 85 N. Gao, Y. Y. Yan, X. Y. Chen and D. J. Mee, *Mater. Lett.*, 2011, **65**, 2902.
- 86 C. Lee and C. J. Kim, *Phys. Rev. Lett.*, 2011, **106**, 014502.
- 87 C. Lee and C. J. Kim, *Langmuir*, 2011, **27**, 4243.
- 88 F. Feuillebois, M. Z. Bazant and O. I. Vinogradova, *Phys. Rev. Lett.*, 2010, **104**, 159902.
- 89 A. Steinberger, C. Cottin-Bizonne, P. Kleimann and E. Charlaix, *Phys. Rev. Lett.*, 2008, **100**, 134501.
- 90 A. Maali, Y. Pan, B. Bhushan and E. Charlaix, *Phys. Rev. E*, 2012, **85**, 066310.
- 91 E. S. Asmolov, A. V. Belyaev and O. I. Vinogradova, *Phys. Rev. E*, 2011, **84**, 026330.
- 92 T. M. Squires and S. R. Quake, *Rev. Modern Phys.*, 2005, **77**, 977.
- 93 S. S. Bahga, O. I. Vinogradova and M. Z. Bazant, *J. Fluid Mechanics*, 2010, **644**, 245.
- 94 A. V. Belyaev and O. I. Vinogradova, *Phys. Rev. Lett.*, 2011, **107**, 098301.
- 95 T. M. Squires, *Phys. Fluids*, 2008, **20**, 092105.
- 96 B. J. Kirby and E. F. Hasselbrink, *Electrophoresis*, 2004, **25**, 187.
- 97 D. M. Huang, C. Cottin-Bizonne, C. Ybert and L. Bocquet, *Phys. Rev. Lett.*, 2008, **101**, 064503.
- 98 P. Roach, N. J. Shirtcliffe and M. I. Newton, *Soft Matter*, 2008, **4**, 224.
- 99 N. J. Shirtcliffe, G. McHale, M. I. Newton and C. C. Perry, *Langmuir*, 2003, **19**, 5626.
- 100 A. Nakajima, A. Fujishima, K. Hashimoto and T. Watanabe, *Adv. Mater.*, 1999, **11**, 1365.
- 101 N. Zhao, F. Shi, Z. Q. Wang and X. Zhang, *Langmuir*, 2005, **21**, 4713.
- 102 M. Nicolas, F. Guittard and S. Geribaldi, *J. Polym. Sci., Part A: Polym. Chem.*, 2007, **45**, 4707.
- 103 H. Yan, K. Kurogi, H. Mayama and K. Tsujii, *Angew. Chem. Int. Ed.*, 2005, **44**, 3453.
- 104 I. Sas, R. E. Gorga, J. A. Joines and K. A. Thoney, *J. Polym. Sci., Part B: Polym. Phys.*, 2012, **50**, 824.
- 105 F. Shi, Y. Y. Song, H. Niu, X. H. Xia, Z. Q. Wang and X. Zhang, *Chem. Mater.*, 2006, **18**, 1365.
- 106 S. S. Latthe, H. Imai, V. Ganesan and A. V. Rao, *Microporous Mesoporous Mater.*, 2010, **130**, 115.
- 107 N. J. Shirtcliffe, G. McHale, M. I. Newton, C. C. Perry and P. Roach, *Chem. Commun.*, 2005, 3135.
- 108 K. Tadanaga, N. Katata and T. Minami, *J. Am. Ceram. Soc.*, 1997, **80**, 3213.
- 109 N. J. Shirtcliffe, G. McHale, M. I. Newton and C. C. Perry, *Langmuir*, 2005, **21**, 937.
- 110 J. Zimmermann, F. A. Reifler, G. Fortunato, L. C. Gerhardt and S. Seeger, *Adv. Funct. Mater.*, 2008, **18**, 3662.
- 111 Y. Horiuchi, Y. Shimizu, T. Kamegawa, K. Mori and H. Yamashita, *Phys. Chem. Chem. Phys.*, 2011, **13**, 6309.
- 112 T. Ishizaki, J. Hieda, N. Saito and O. Takai, *Electrochim. Acta*, 2010, **55**, 7094.
- 113 M. Miwa, A. Nakajima, A. Fujishima, K. Hashimoto and T. Watanabe, *Langmuir*, 2000, **16**, 5754.
- 114 F. Shi, X. X. Chen, L. Y. Wang, J. Niu, J. H. Yu, Z. Q. Wang and X. Zhang, *Chem. Mater.*, 2005, **17**, 6177.
- 115 T. Baldacchini, J. E. Carey, M. Zhou and E. Mazur, *Langmuir*, 2006, **22**, 4917.
- 116 J. Rafiee, M. A. Rafiee, Z. Z. Yu and N. Koratkar, *Adv. Mater.*, 2010, **22**, 2151.
- 117 L. Feng, S. H. Li, H. J. Li, J. Zhai, Y. L. Song, L. Jiang and D. B. Zhu, *Angew. Chem. Int. Ed.*, 2002, **41**, 1221.
- 118 J. C. McDonald, D. C. Duffy, J. R. Anderson, D. T. Chiu, H. K. Wu, O. J. A. Schueller and G. M. Whitesides, *Electrophoresis*, 2000, **21**, 27.
- 119 J. C. McDonald and G. M. Whitesides, *Acc. Chem. Res.*, 2002, **35**, 491.
- 120 J. N. Lee, C. Park and G. M. Whitesides, *Anal. Chem.*, 2003, **75**, 6544.
- 121 A. Pozzato, S. Dal Zilio, G. Fois, D. Vendramin, G. Mistura, M. Belotti, Y. Chen and M. Natali, *Microelectron. Eng.*, 2006, **83**, 884.
- 122 R. Pogreb, G. Whyman, R. Barayev, E. Bormashenko and D. Aurbach, *Appl. Phys. Lett.*, 2009, **94**, 221902.
- 123 B. D. Gates, Q. B. Xu, M. Stewart, D. Ryan, C. G. Willson and G. M. Whitesides, *Chem. Rev.*, 2005, **105**, 1171.
- 124 C. Peroz, C. Heitz, E. Barthel, E. Sondergard and V. Goletto, *J. Vacuum Sci. Technol. B*, 2007, **25**, L27.
- 125 C. Peroz, V. Chauveau, E. Barthel and E. Sondergard, *Adv. Mater.*, 2009, **21**, 555.
- 126 A. Letailleur, J. Teisseire, N. Chemin, E. Barthel and E. Sondergard, *Chem. Mater.*, 2010, **22**, 3143.
- 127 M. Reyssat, F. Pardo and D. Quere, *EPL*, 2009, **87**, 5.
- 128 D. G. Choi, J. H. Jeong, Y. S. Sim, E. S. Lee, W. S. Kim and B. S. Bae, *Langmuir*, 2005, **21**, 9390.
- 129 J. C. Love, L. A. Estroff, J. K. Kriebel, R. G. Nuzzo and G. M. Whitesides, *Chem. Rev.*, 2005, **105**, 1103.
- 130 E. Hosono, S. Fujihara, I. Honma and H. S. Zhou, *J. Am. Chem. Soc.*, 2005, **127**, 13458.

Received: 24th July 2012; Com. 12/3959